Full-sun temperature distribution and classification of coronal structures

Noriyuki Narukage,[1*] Masumi Shimojo,[2] Taro Sakao,[1] Ryouhei Kano,[3]
Kiyoto Shibasaki,[2] Edward E. DeLuca,[4] Mark A. Weber,[4]
Steven H. Saar,[4] Patricia R. Jibben,[4] Saku Tsuneta[3]

[1]Institute of Space and Astronautical Science, Japan Aerospace Exploration Agency,
Sagamihara, Kanagawa 229-8510, Japan
[2]Nobeyama Solar Radio Observatory, National Astronomical Observatory of Japan,
Nobeyama, Nagano, 384-1305, Japan
[3]National Astronomical Observatory of Japan,
Mitaka, Tokyo, 181-8588, Japan
[4]Smithsonian Astrophysical Observatory,
60 Garden Street, Cambridge, MA 02138, United States

[*]To whom correspondence should be addressed; E-mail: narukage@solar.isas.jaxa.jp.

Coronal observations in X-rays show the sun has many dynamic features that can neither be imagined nor seen with the naked eye. The solar corona has a wide temperature range from less than 1MK (1,000,000K) to more than 10MK. The X-ray telescope (XRT) on board the *Hinode* satellite has 9 X-ray analysis filters to observe the almost of whole coronal plasma. Using the data observed with this telescope, we successfully derived the coronal temperature around the whole sun. We also found that coronal structures are nicely classified using the temperature and emission measure. Furthermore, the coronal structures were found to depend on the length of structure and the heating flux. This

might be the great clue to solving the big coronal heating question.

In the solar corona, there are many kind of features. An active region is a bright region in X-rays where energy gets released, namely by solar flares and transient brightenings. So, typically active regions are composed of hot plasma. However, most of the sun is relatively quiet and then called quiet region. The darkest region in X-rays is a coronal hole, where the magnetic fields are open and the coronal plasma is flowing out to interplanetary space.

The soft X-ray telescope (SXT) (*1*) on board *Yohkoh* satellite (*2*) had provided many beautiful coronal images during more than 10 years of operation (1991–2001). This telescope had an ability to determine coronal plasma temperatures of more than 2MK (*3, 4*). So SXT was a useful tool for examining the energetics in the solar corona. However, SXT was not sensitive to cool plasmas ($<$ 2MK) and could not adequately observe the low-energetic regions, e.g., quiet region or coronal hole. On 23 September 2006, a new solar observing satellite, *Hinode* (*5*), was launched. One of the three telescope systems aboard *Hinode* is the X-ray telescope (XRT) (*6, 7*) which is the successor of SXT. The XRT has 9 X-ray analysis filters with different temperature responses to cover the temperature range from less than 1MK to more than 10MK. This means that the XRT can observe the almost of whole coronal plasma.

The purpose of this paper is to derive the coronal temperature around the whole sun using superior X-ray telescope, and to examine how the coronal temperature is distributed. Then we find that the coronal structures are nicely classified with the temperature and emission measure. Based on the energy balance theory, this result shows that the coronal structures are determined with the length of structure and heating flux.

On 22 February 2007, XRT took full-sun images with both thin Al mesh and Ti poly filters. These observations are used in this paper. The thin Al mesh filter is the thinnest filter and has a peak sensitivity to 1–3MK plasma. Meanwhile, the Ti poly filter can mainly detect 2–5MK plasma. XRT has high contrast and low CCD noise, so the temperature can be derived for not

only bright active regions but also relatively dark quiet regions and coronal holes. The spatial resolution of the XRT is 1 arcsec ($\sim$ 730 km on the solar disk) yielding a highly resolved temperature map. More details about XRT can be found in the instrumental papers (*6, 7*).

For the observations analyzed in this paper, we took images with relatively short and long exposure in each filters to adequately resolve both bright and dim features. The exposure times are 0.5 & 4 sec for the thin Al mesh filter and 1 & 8 sec for the Ti poly filter.

Fig. 1 shows the full-sun image and derived coronal temperature. Fig. 1-A indicates the solar X-ray image taken with thin Al mesh filter at 00:02 on 22 February 2007. Near the center of the sun is a bright active region with two dark coronal holes (dark patches). Most of the sun is relatively quiet and called a quiet region. Each coronal structure emits X-rays at different intensity levels. The X-ray emission is proportional to the square of the coronal electron number density n, when the temperature is constant. Then, the emission measure, EM, is defined as the index of emission: $EM \equiv fn^2l$ [cm^{-5}], where f is the filling factor defined as the ratio of the coronal volume radiating in X-rays to the total volume, and l is the line-of-sight length of the coronal structure, which is roughly equal to the height of the coronal structure. Using this EM, the intensity observed with a certain filter is described as $I = R(T) \cdot EM$, where $R(T)$ is the temperature response of a filter and T is temperature. Each filter has each $R(T)$ which depends on the material and thickness of each filter, and is known quantity measured in the laboratory.

Applying this to the observations we get the intensities I_{Al} ($= R_{Al}(T) \cdot EM$) and I_{Ti} ($= R_{Ti}(T) \cdot EM$) for the thin Al mesh filter and the Ti poly filter, respectively. Taking the ratio of these two intensities, we obtain the following relation: $I_{Ti}/I_{Al} = R_{Ti}(T)/R_{Al}(T)$. The right hand side of this relation is known measured properties of the filters themselves and it depends on temperature of the observed plasma. Therefore, the coronal temperatures can be derived using just 2 filters (*8, 9*). We note that the temperature derived this method (called "filter ratio method") represents the mean temperature biased by the 2 filters. Fig. 1-B is the

coronal temperature distribution derived with the X-ray data taken with Al-mesh and Ti-poly filter. Using these 2 filters, we can derive the temperature in the range between 1MK and 5MK. Hence these two filters are a suitable pair to examine a full-sun temperature distribution, because the typical temperature of features like: coronal holes, quiet regions and active regions are $\sim$1MK, $\sim$2MK and $>$3MK, respectively.

Once the temperature is derived, the emission measure can also be obtained. Fig. 2-A shows the relationship between the temperature and emission measure (temperature-emission measure (T-EM) diagram) derived with the data shown in Fig. 1. To reduce the line-of-sight effect, we only included data points which are located near the disk center ($a > 60$ degree, where a is the angle between the line-of-sight direction and radial direction of the data point). In Fig. 2-A, we can see the general trend shown by the dashed gray lines in Fig. 2-B. These lines represent the relation $EM \propto T^4$. This relation can be explained by considering the energy balance in the corona. If the heating time becomes sufficiently long, the heating flux (H), conductive flux (F_C) and radiative flux (F_R) are all comparable (*10*). In the solar corona, these are described as follows :

$$H \simeq F_C \simeq F_R, \tag{1}$$

$$F_C = \frac{d}{dl}\left(\kappa \frac{d}{dl} T\right) l \approx 9.0 \times 10^{-7} l^{-1} T^{7/2}, \tag{2}$$

$$F_R = n^2 Q\left(T\right) l \approx 9.5 \times 10^{-20} n^2 l T^{-1/2}, \tag{3}$$

, where $\kappa \approx 9.0 \times 10^{-7} T^{5/2}$ is the Spitzer thermal conductivity (*11*), $Q\left(T\right)$ is the radiative loss function approximating to $Q\left(T\right) \approx 3 \times 10^{-23} (T/10^7)^{-1/2}$ for $10^6 < T < 10^7$ K. To substitute equations (2) and (3) for (1), we can obtain the following relation: $n \approx 3.1 \times 10^6 l^{-1} T^2$. Note that this is basically the same as the scaling law of Rosner-Tucker-Vaiana [$T \propto (pL)^{1/3}$] (*10*), where p and L are pressure and length of structure, respectively. Based on the definition of EM

($\equiv fn^2l$), this relation is rewritten as

$$EM \approx 9.5 \times 10^{12} f l^{-1} T^4. \tag{4}$$

The dashed gray lines in Fig. 2-B represent this relation. The difference of each line is due to the difference of the length l. The values of l are described near each dashed line, where we assume $f = 0.1$.

In the sun, the hot 1MK corona stably exists above the cool 6,000K solar surface (*12*). This means that the corona is continuously heated. However, such coronal heating mechanism is still a mystery and one of the biggest puzzles in solar physics. To solve this puzzle, the estimation of the heating flux is indispensable. Hence, we consider the dependence of the heating flux H on the T-EM diagram. Using the relation in equation (1) as $H \sim F_C$ and equation (2), the length of structure is described as $l = 9.0 \times 10^{-7} H^{-1} T^{7/2}$. To substitute this for equation (4), we can obtain the T-EM relation depending on the heating flux:

$$EM \approx 1.1 \times 10^{19} f H T^{1/2}. \tag{5}$$

This relation is indicated by solid gray lines in Fig. 2-B. The figures near each solid line show the values of H, where we assume $f = 0.1$.

The T-EM diagram is divided into areas by the dashed and solid gray lines in Fig. 2-B. Finally, we examined where the data points in each area is distributed on the sun. Fig. 3 shows the distribution of the data points. Each color in Fig. 3 corresponds to the color in Fig. 2-B. Based on Fig. 1-A, 2 and 3, we found that the coronal structures are nicely classified with the T-EM diagrams, and we can conclude that the coronal structures are determined with the length of the structure and heating flux. These results are summarized in Table 1. Here we also assumed that the filling factor is 0.1.

We could successfully derive the full-sun temperature distribution using only one data set, typically consisting of 4 different-filter and different-exposure images as described above, ow-

ing to the superior capability of the XRT for both quiet sun and active region observations. This means that the XRT makes us possible to derive the coronal temperature anywhere and to examine the time evolution of coronal temperature (see the attached movie).

In this paper, we directed our attention to the relation between the coronal structures and their temperature. Based on the full-sun temperature distribution derived with XRT, we found that coronal structures are nicely classified in the T-EM diagram. In previous works, the relationship between the temperature and emission measure had been examined, but only for flares and active regions where X-rays are strongly emitted and the $T > 2$MK (*13–15*), or for the outside of the solar disk (*16*). This is the first time that temperatures < 2MK (colored blue or purple in Fig. 1-B) have been examined in detail. In the T-EM diagram (Fig. 2), the data points distributed in left half ($\log_{10}(T) < \log_{10}(2\mathrm{MK}) = 6.3$) are first to ever be analyzed. From these results, it is obvious that the XRT is a powerful tool to examine the physics in the solar corona.

Furthermore, we discovered that the coronal structures are determined by the length of the coronal structure and the heating flux. The derived heating flux agrees with the previous works at the temperature range of $T > 2$MK (*17, 18*). A detailed comparison between the heating flux derived from this work and the corresponding magnetic field should provide us with further insights for unraveling the mystery of coronal heating.

References and Notes

1. S. Tsuneta, L. W. Acton, M. Bruner, J. Lemen, W. Brown, R. Caravalho, R. Catura, S. Freeland, et al., *Sol. Phys.* **136**, 37 (1991).
2. Y. Ogawara, T. Tanaka, T. Kato, T. Kosugi, S. Tsuneta, T. Watanabe, I. Kondo and Y. Uchida, *Sol. Phys.* **136**, 1 (1991).
3. H. Hara, S. Tsuneta, J. R. Lemen, L. W. Acton and J. M. McTiernan, *PASJ* **44**, 135 (1992).

4. T. Yoshida, S. Tsuneta, L. Golub, K. Strong and Y. Ogawara, *PASJ* **47**, 15 (1995).
5. T. Kosugi, et al., *Sol. Phys.* in press (2007).
6. L. Golub, et al., *Sol. Phys.* in press (2007).
7. R. Kano, et al., *Sol. Phys.* in press (2007).
8. G. S. Vaiana, A. S. Krieger and A. F. Timothy, *Sol. Phys.* **32**, 81 (1973).
9. M. Gerassimenko and J. T. Nolte, *Sol. Phys.* **60**, 299 (1978).
10. R. Rosner, W. H. Tucker and G. S. Vaiana, *ApJ* **220**, 643 (1978).
11. L. Spitzer Jr., *Physics of Fully Ionized Gases* (New York: Interscience, 1956).
12. C. H. Mandrini, P. Démoulin and J. A. Klimchuk, *ApJ* **530**, 999 (2000).
13. T. Yoshida and S. Tsuneta, *ApJ* **459**, 342 (1996).
14. K. Shibata and T. Yokoyama, *ApJ* **562**, 49 (1999).
15. K. Shibata and T. Yokoyama, *ApJ* **577**, 422 (2002).
16. M. J. Aschwanden and L. W. Acton, *ApJ* **550**, 475 (2001).
17. G. L. Withbroe and R. W. Noyes, *ARAA* **15**, 363 (1977).
18. M. J. Aschwanden, *ApJ* **560**, 1035 (2001).

Hinode is a Japanese mission developed and launched by ISAS/JAXA, collaborating with NAOJ as a domestic partner, NASA and STFC (UK) as international partners. Scientific operation of the *Hinode* mission is conducted by the *Hinode* science team organized at ISAS/JAXA. This team mainly consists of scientists from institutes in the partner countries. Support for the post-launch operation is provided by JAXA and NAOJ (Japan), STFC (U.K.), NASA, ESA, and NSC (Norway).

We wish to express our sincere gratitude to late Prof. Takeo Kosugi, former project manager of *Hinode* at ISAS, who passed away all of a sudden in November 2006. Without his leadership in the development of *Solar-B* / *Hinode*, this mission would have never been realized.

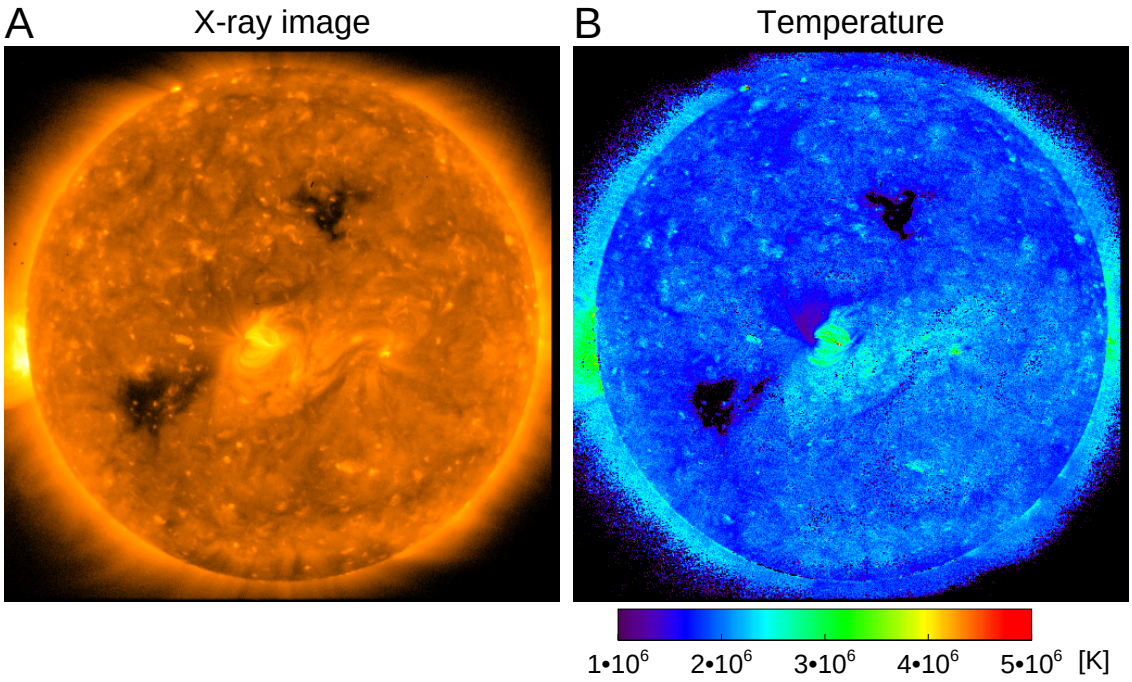

Fig. 1. Full-sun image and derived coronal temperature. Fig. 1-A is an X-ray image of the sun taken with thin Al mesh filter at 00:02 on 22 February 2007. This is a composite image with short and long exposure images, where saturated pixels in the longer exposure image were replaced with the shorter exposure image pixels. So you can clearly see the various coronal structures emitting at very different intensity levels. Fig. 1-B is the coronal temperature distribution derived with the X-ray data taken with Al-mesh and Ti-poly filter. The different colors represent the temperature (see color bar). The black-colored region indicates the unmeasurable region because of the low coronal emission there. Such regions have more than 20% signal to noise or more than 20% error in derived temperature. The spacial resolution of the temperature distribution is 1–3 arcsec (cf. the resolution of the X-ray image is 1 arcsec), because we sum up the intensity in 2×2 or 3×3 pixels to reduce the photon noise ($< 20\%$) in the low-intensity regions.

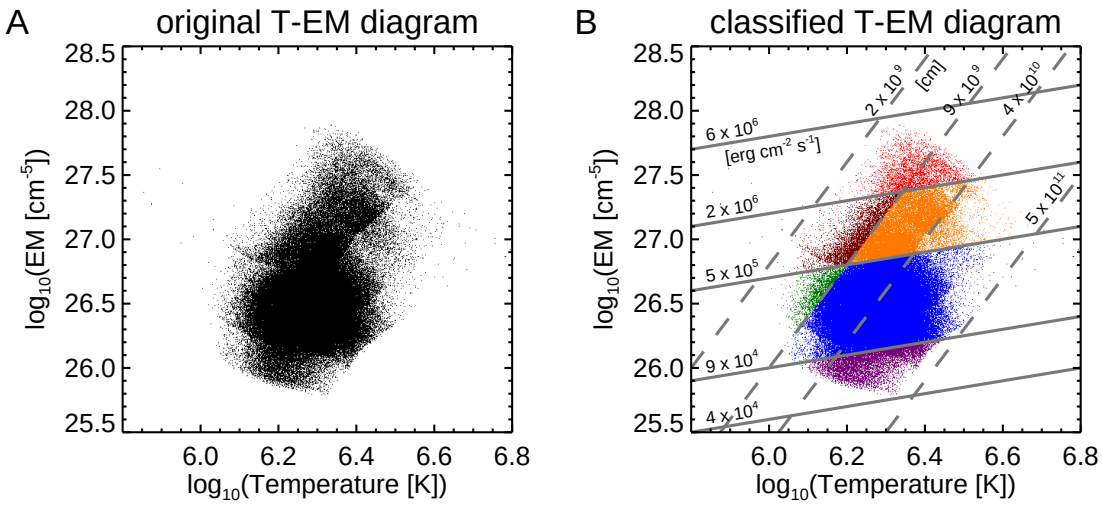

Fig. 2. Relation between the temperature and emission measure (temperature-emission measure (T-EM) diagram). Fig. 2-A is the original diagram. Fig. 2-B is the diagram classified with dashed and solid gray lines. The dashed gray lines represent the relation $EM \propto T^4$ and the figures near each line show the values of l, where we assume $f = 0.1$. Meanwhile, the solid gray lines represent the relation $EM \propto T^{1/2}$ and the figures show the values of H, where we also assume $f = 0.1$.

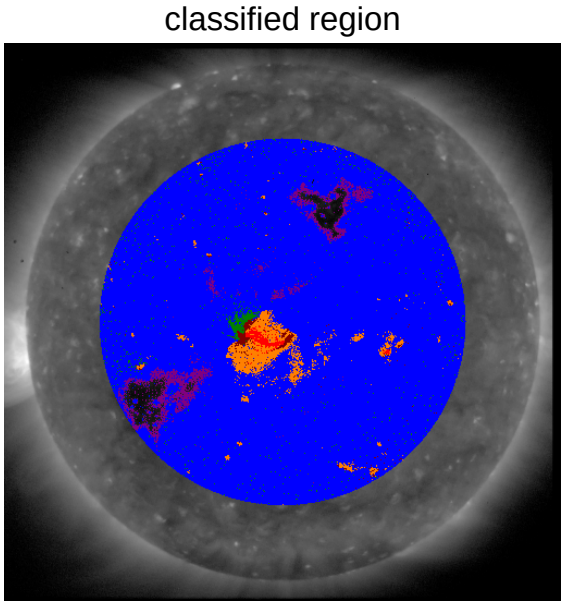

Fig. 3. Classified region with T-EM diagram. In comparison with Fig. 1-A, red is located in the core of the active region, orange represents the outer active region (AR) as well as X-ray bright point (XBP). Brown appears around the foot points of active region loops and blue is most of the quiet region, while purple is the coronal hole. The green area near the active region is an area where XRT observed plasma flowing from the AR. Colors correspond to data point colors in Fig. 2-B.

Table 1: Coronal structure and associated length & heating flux

Coronal structure	Length [cm]	Heating flux [erg cm^{-2} s^{-1}]	Color in Fig. 3
Active region core	$2 \times 10^9 - 4 \times 10^{10}$	$2 \times 10^6 - 6 \times 10^6$	red
Active region & XBP	$9 \times 10^9 - 4 \times 10^{10}$	$5 \times 10^5 - 2 \times 10^6$	orange
Around foot point	$2 \times 10^9 - 9 \times 10^9$	$5 \times 10^5 - 2 \times 10^6$	brown
Quiet region	$9 \times 10^9 - 5 \times 10^{11}$	$9 \times 10^4 - 5 \times 10^5$	blue
Plasma flow from AR	$2 \times 10^9 - 9 \times 10^9$	$9 \times 10^4 - 5 \times 10^5$	green
Coronal hole	$4 \times 10^{10} - 5 \times 10^{11}$	$4 \times 10^4 - 9 \times 10^4$	purple

$*$ Here we assume $f = 0.1$.